Development and Experimental Verification of the Wide-Aperture Catheter-Based Microwave Cardiac Ablation Antenna

Zeji Gu, Carey M. Rappaport, *Senior Member, IEEE*, Paul J. Wang, and Brian A. VanderBrink

***Abstract*—A new type of catheter-based microwave antenna cardiac ablation applicator has been developed. Unlike previously developed ablation catheters, this device forms a wide aperture that produces a large heating pattern. The antenna consists of the center conductor of a coaxial line, shaped into a spiral and insulated from blood and tissue by a nonconductive fluid-filled balloon. The antenna will be stretched straight inside a catheter for transluminal guiding. Once in place at the cardiac target, the balloon will be inflated, and the coiled spiral antenna will be ejected into the inflated balloon. The wide aperture antenna generates a ring-shaped power pattern. The heat generated from this deposited power is conducted through a volume larger than the spiral diameter, ablating diseased tissue. The resultant lesion profile is both wider and deeper than that of either conventionally used RF catheter-based ablation electrodes or that of other recently reported microwave applicators, and may offer greater heating accuracy and controllability. The new antenna design is tested by measuring S_{11}- and S_{21}-parameters, and by comparing power deposition patterns to conventional monopole antenna in a tissue-equivalent phantom. Heating experiments on *in vitro* organ tissue and on live pigs using 50, 100, and 150 W of 915-MHz microwave power have been performed to test the efficacy of the wide-aperture antenna design. These studies confirm the hypotheses that the wide-aperture microwave antenna can create lesions of significant depth that may be applicable for the ablative therapy of ventricular tachycardia.**

***Index Terms*—Biomedical devices, microwave heating, wire antennas.**

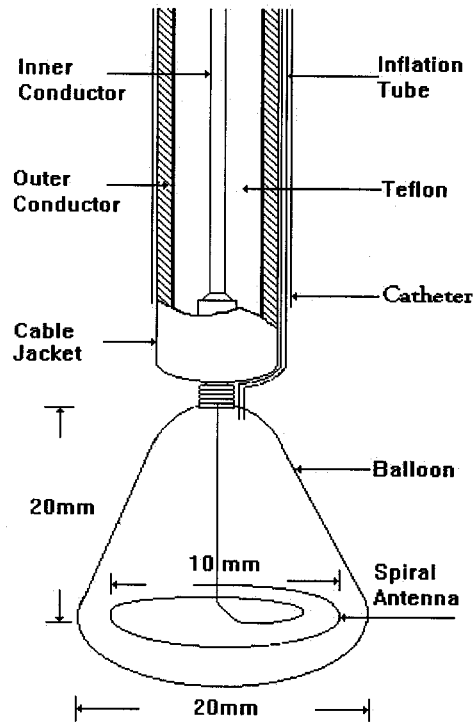

Fig. 1. Schematic view of the wide-aperture microwave ablation catheter and tip showing the structure of the coaxial cable, spiral antenna, and the balloon.

I. Introduction

Treating cardiac arrhythmias with electromagnetically generated heat is becoming widely accepted. RF ablation is an important alternative to pharmacologic treatment, with high success rates in treating a wide range of atrial and ventricular cardiac arrhythmias [1]–[3]. A similar high success rate has unfortunately not been achieved in patients with ventricular tachycardia [4], [5]. Failure to cure ventricular tachycardia associated with coronary artery disease has been attributed to the small lesion size produced with currently available RF ablation catheters. Increasing the power applied to heat tissue at depth often results in excessive temperature at the electrode–tissue interface without the desired enlargement of lesion size. Since desiccation of tissue causes an abrupt rise in impedance and limits energy transfer to the tissue [6], it is believed that the maximum effective depth of the ablated cardiac tissue with the RF method is approximately 0.5 cm. However, in the typical case, the myocardial infarction lies much deeper in the ventricular myocardium [7]. In addition, it has been suggested that the zone of slow conduction mediating reentrant ventricular tachycardia may be up to several square centimeters in size [8]. Technologies capable of safely heating such a large volume of tissue, such as those employing microwave energy, may be well suited for ablation of ventricular tachycardia. In contrast to heating by electrical resistance as observed during RF ablation, heating with microwaves is due to a propagating electromagnetic field that raises the energy of the dielectric molecules through which the field passes by both conduction and displacement currents. Thus, in microwave ablation, the initial volume of ablation is a result of direct electromagnetically induced dielectric frictional

Manuscript received November 15, 1999; revised April 24, 2000. This work was supported by The Whitaker Foundation under the Biomedical Engineering Research Grant Program.

Z. Gu was with the Department of Electrical and Computer Engineering, Northeastern University, Boston, MA 02115 USA. He is now with Alpha Industries Inc., Woburn, MA 01801 USA.

C. M. Rappaport is with the Department of Electrical and Computer Engineering, Northeastern University, Boston, MA 02115 USA.

P. J. Wang and B. A. VanderBrink are with the New England Medical Center Hospital, Boston, MA 02111 USA.

Publisher Item Identifier S 0018-9480(00)09551-X.

0018–9480/00$10.00 © 2000 IEEE

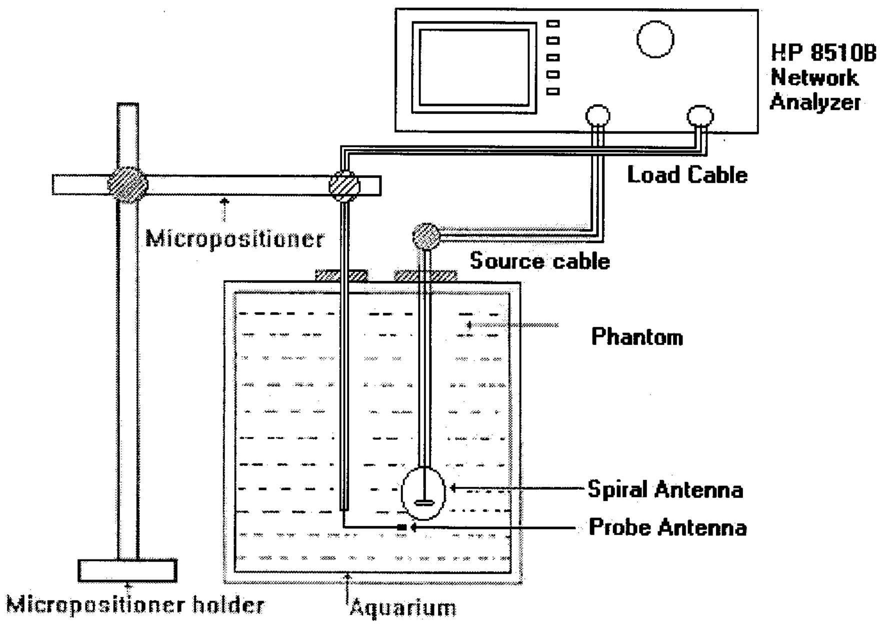

Fig. 2. Experimental setup for measuring the reflection coefficient S_{11} and transmission coefficient S_{21} by the spiral antenna embedded in the phantom.

heating and is unlikely to be limited by local tissue factors or electrode size. This mode of heating lends microwave ablation the potential for a greater depth and larger volume heating than RF ablation and should result in a larger lesion size [9], [10]. Previous research has shown that lesions created by microwave energy increase in size with increased applied power [11].

Microwave catheter-based antenna applicators have been used experimentally for cardiac ablation. These applicators may be grouped into two categories: the monopolar antennas [12], [13] and helical coil antennas [6], [14], [15]. The monopolar antennas are usually one-half tissue wavelength long, designed to radiate in the normal mode to generate a well-defined football-shaped heating pattern along the antenna length. The helical coil antenna applicator is also designed to radiate in the normal mode, perpendicular to the axis of the helix. The helix has been shown to exhibit improved uniformity and localization of heating along the radiating coil portion of the antenna compared to the monopole configuration.

It is desirable, however, to have an illuminating aperture that is as large as possible. The monopole and helix antenna applicators have radiating apertures limited by the diameters of their catheters, and as such must be often be repositioned to create a sufficiently large lesion [16]. The purpose of this paper is to propose a wide aperture antenna design by using a spiral antenna covered by a balloon, and to demonstrate the feasibility by comparison with conventional monopole applicator in phantom medium and *in vitro* and *in vivo* tests with various microwave energy delivery.

II. Antenna Applicator Design

Unlike monopole antennas, which radiate normal to their axes, and conventional RF electrodes, which generate radial currents, loop antennas can radiate in either normal or axial modes. Electrically small current loops behave like magnetic dipoles, with the electric field strongest in the plane of the loop and polarized circumferentially. However, once the loop circumference approaches one wavelength (in the medium surrounding the loop), the waves it radiates are strongest in the axial direction, with a rotating electric field polarized perpendicular to this axis. With proper loop radius adjustment and surrounding medium specification, it is possible to tailor the radiation pattern, creating a ring of deposited power. Thermal conduction then “fills in” the ring, providing a hemi-oblate spheroid lesion shape.

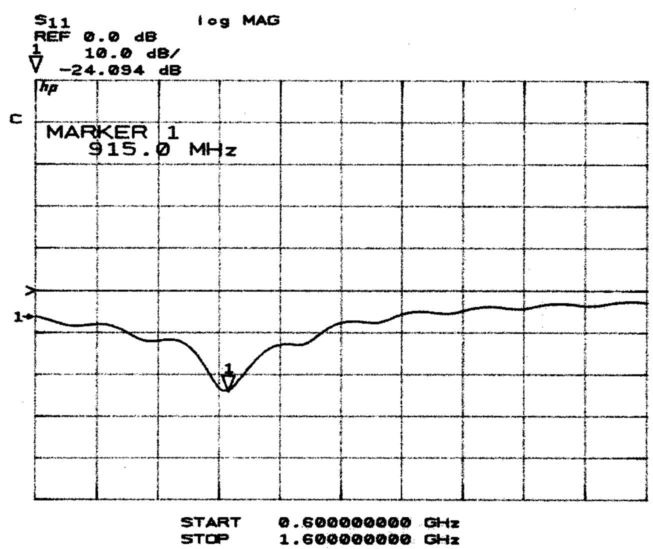

Fig. 3. Measured reflection coefficient as a function of frequency for the wide-aperture spiral antenna in a heart equivalent liquid phantom.

An important aspect of the antenna applicator design is matching of the impedance from applicator to tissue. In practice, an unfurlable spiral formed from the extended center conductor of a coaxial feed line is used instead of a loop. The

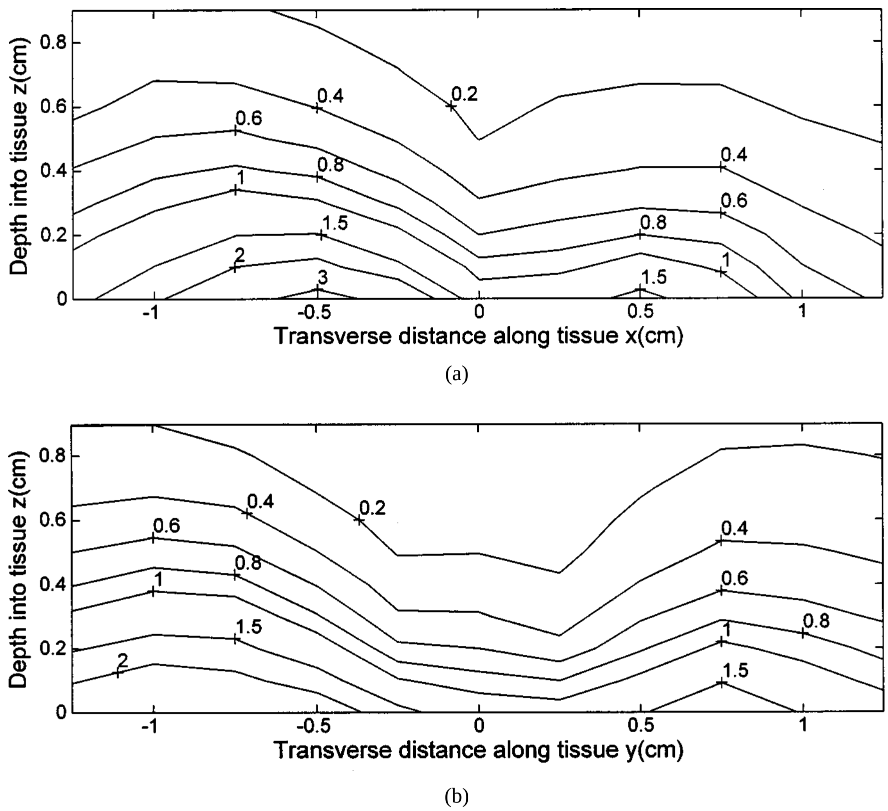

Fig. 4. Measured relative deposition power contour plot for spiral antenna asymmetrically surrounded by insulator-filled balloon immersed in phantom on: (a) $x-z$-plane and (b) y–z-plane, $b=0.5$ cm, $c=1$ cm. Loop shift distance $l/c=0.87$. $S_{11}=-24.1$ dB.

spiral will be introduced through blood vessels into the heart chamber in a compact collapsed state and then ejected from a catheter housing and allowed to reform a spiral shape. Fig. 1 shows this geometry, with balloon inflated and spiral unfurled. It was experimentally determined that the overall length of the center conductor wire governs the antenna impedance. Previous experiments [17] demonstrated that about a one tissue wavelength provided the best match to the 50-Ω coaxial cable.

To first order, it is possible to approximately model the spiral antenna as a circular loop. This model gives a sense of the power deposition pattern and, thus, the heating profiles. For a one-wavelength circumference loop, current on one side of the loop will be 180° out of phase and flow in the opposite direction from that on the diametrically opposite side. Thus, these two currents will excite fields that constructively interfere along the axis of the loop and cancel outside the loop. For a loop positioned on a planar tissue surface, this modest focusing yields an enhanced electric field and, hence, increased power deposition at depth within the tissue. In high water content tissue, one wavelength corresponds to 4.5 cm at 915 MHz [18], which establishes a nominal loop diameter of 1.4 cm.

It was determined experimentally that to produce the desired size lesion of slightly greater than 1-cm diameter and prevent tissue surface overheating, an inner region of low-loss low-dielectric-constant fluid surrounding the spiral was needed. This physiologically benign fluid—usually air, nitrogen, or a perfluorocarbon blood substitute—is contained within a balloon surrounding the loop. An inflation tube is used to fill and drain the fluid. For therapeutic purposes, it is preferable to direct the radiated power directly into the cardiac tissue. Not only does this

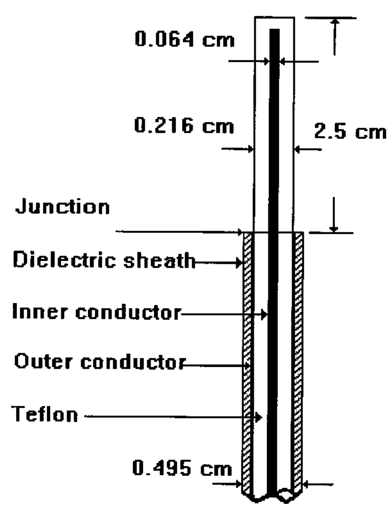

Fig. 5. Schematic view of a bare monopole microwave antenna, used as an experimental reference.

prevent heating of blood within the heart chamber, it also delivers more of the available power into the heart tissue. Directing the power flow is achieved by asymmetrically positioning the loop in an inflatable balloon, with less fluid in front of the loop than behind it. The loop antenna is specified with radius b placed eccentrically inside the balloon with radius c, in a plane at a distance l from the center of the balloon. For the spiral within a balloon, the simple model of a single-wavelength circumference loop breaks down, and a more sophisticated moment-method analysis is required. Repeated experimental and numerical trials

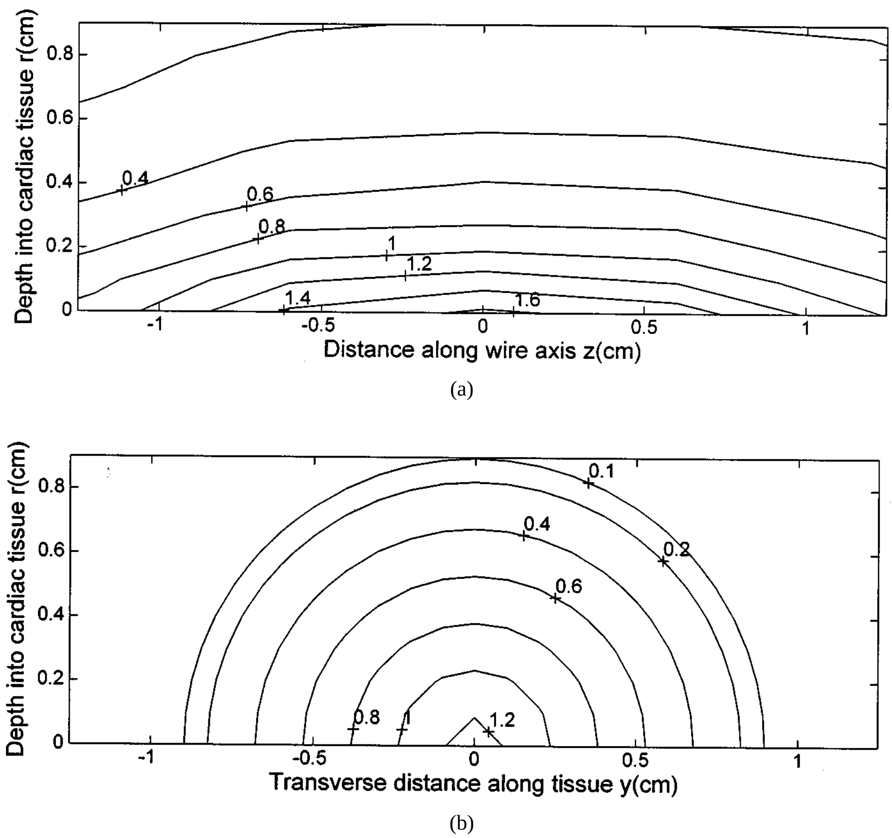

Fig. 6. Measured deposition power contour plot for bare monopole antenna immersed in phantom, with length 2.5 cm, on: (a) z–ρ-plane and (b) y–ρ-plane

concluded that a smaller diameter spiral performs better in the balloon-enclosed environment. The best radius was found to be $b = 0.5$ cm (about 70% of the nominal radius) with balloon radius $c = 1$ cm.

III. Experiments and Results

To validate the new wide-aperture spiral antenna applicator and define the characteristics of microwave heating in myocardial tissue, phantom tests and *in vitro* tissue tests, as well as *in vivo* living animal tests were performed.

The wide-aperture spiral antenna was built from a coaxial RG 58 cable, chosen for its high power-handling capability and ease of fabrication of the spiral antenna. The cable jacket and outer conductor were stripped to a length of 4.5 cm, the Teflon insulator was thinned, and this active segment was then curved into a spiral with about 1-1/4 turns. The coaxial cable was sealed at the antenna end. A tube capable of inflating a balloon was introduced parallel to the coaxial line. The spiral and inflation tube were surrounded by the balloon and firmly sealed with silicon rubber adhesive. The total catheter length was chosen to be 100 cm.

A. Low-Power Phantom Tests

Before the antenna was used for ablation, it was tested in an artificial blood/heart tissue phantom for microwave frequencies in the range from 600 to 1600 MHz using an HP 8510B microwave network analyzer, as shown schematically in Fig. 2. The phantom consisted of a saline/sucrose solution, mixed in proportions based on standard recipes, to model the electromagnetic characteristics of high-water-content tissue—such as cardiac tissue and blood—at 915 MHz: the dielectric constant is 51 and electrical conductivity is 1.3 S/m [18]. Measurements of S_{11} were performed with the antenna embedded in the phantom. The antenna penetrated at least 10 cm below the surface to eliminate the dielectric mismatch at the air–phantom interface. The antenna input was mated to the source port of the network analyzer.

Fig. 3 shows the magnitude of the measured reflection coefficient S_{11} of the antenna embedded in the phantom. At the operating frequency of 915 MHz, the value of S_{11} is -24.1 dB, corresponding to 99.6% of the power supplied being radiated from the antenna and absorbed in the feeding cable. Thus, it can be concluded that the antenna couples quite well to the biological tissue at 915 MHz.

The transmitted power deposition was measured by using a simple short monopole probe antenna, which sampled the electric field at various locations within the phantom. An inherent and unavoidable limitation of this procedure is that the probe antenna must be very small for high-resolution measurements, but in being so small, it couples poorly to the phantom. Field readings are, therefore, relative rather than absolute. The probe antenna consists of a coaxial cable with 10 mm of the center conductor extended beyond the outer conductor. The probe can only measure the phase and amplitude of a single polarization of the electric field. The squared magnitudes of all electric-field polarizations are summed to determine the relative deposited power pattern in the phantom. The spiral antenna and monopole probe are modeled as a two-port network. According to two-port network theory, the S_{11} gives a measure of how well the antenna radiates power into phantom, while S_{21} represents how

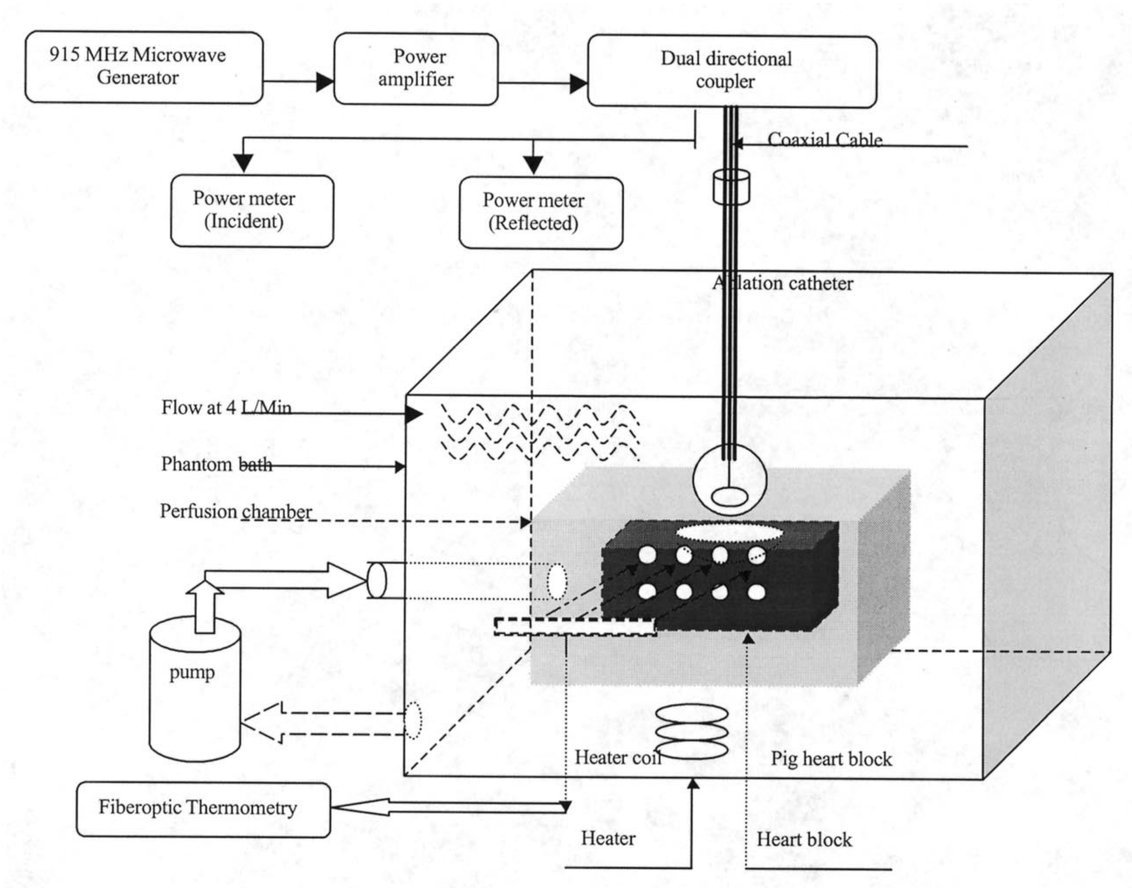

Fig. 7. Perfused pig heart model for evaluation of cardiac ablation catheter. The catheter to be evaluated is placed on the surface of the pig heart, immersed in a perfused chamber. Cardiac perfusion is simulated by pumping phantom fluid across tissue block.

well the power is transferred between the two antennas through the phantom.

Fig. 4 shows the measured power deposition contours given by squaring the magnitude of S_{21}. For the purpose of these plots, the spiral is oriented so that its axis is facing the forward z-direction. Fig. 4(a) gives the pattern in the x–z-plane, which includes the feed line, along the negative x-direction, while Fig. 4(b) shows the pattern in the y–z-plane.

The above results can be compared with those obtained with a simple monopole antenna. A monopole with geometry shown in Fig. 5 was fabricated and measured in the same phantom setup previously used. The center conductor, pointing in the z-direction parallel and against the tissue surface, extends 2.5 cm, or slightly more than one-half a tissue wavelength. Contour plots for the resulting deposited power patterns are shown in Fig. 6. Fig. 6(a) shows the power pattern in the z–ρ-plane, where the ρ-direction points into the tissue, while Fig. 6(b) gives the circularly symmetric pattern in the plane perpendicular to the monopole axis.

Comparing the measured relative power deposition patterns for the spiral and monopole antennas indicates the superiority of the former in heating tissue to form well-defined lesions. Whereas the monopole pattern is widely spread along the 2.5-cm wire length, it is narrow in the transverse direction perpendicular to the wire, and power levels fall off relatively quickly with depth into the tissue. The spiral antenna, on the other hand, deposits more of its power in a ring near the axis of the spiral. The spiral antenna pattern is more nearly toroidal and is deeper than the monopole antenna pattern.

B. In Vitro Tissue Tests

Microwave heating was tested using a custom-built 915-MHz power source with output power level adjustable from 0.001 to 330 W and duration adjustable from 1 s to 99 min. Forward and backward power were monitored throughout the course of each heating experiment. The transmitted power was set to three levels for testing (50, 100, and 150 W), the duration was set at 60 s, and the forward and reflected power was recorded in each case. The antenna was positioned with the antenna axis perpendicular to the surface of the medium to be heated. A fulcrum balanced the weight of the antenna and assured constant tissue pressure. All *in vitro* and *in vivo* temperature measurements were performed with the fluoroptic thermometry system (Luxtron model 790, measurement range, -200 °C to 450 °C, accuracy ± 0.1 °C Luxtron Corporation, Santa Clara, CA). Prior to each application, 10 cm^3 of room air inflated the balloon surrounding the spiral antenna. During each application of microwave energy, the power and fluoroptic temperature probes were continuously monitored and recorded.

In vitro experiments were performed in isolated perfused pig hearts to identify how much power would be required to effectively ablate myocardial tissue and to demonstrate the time course

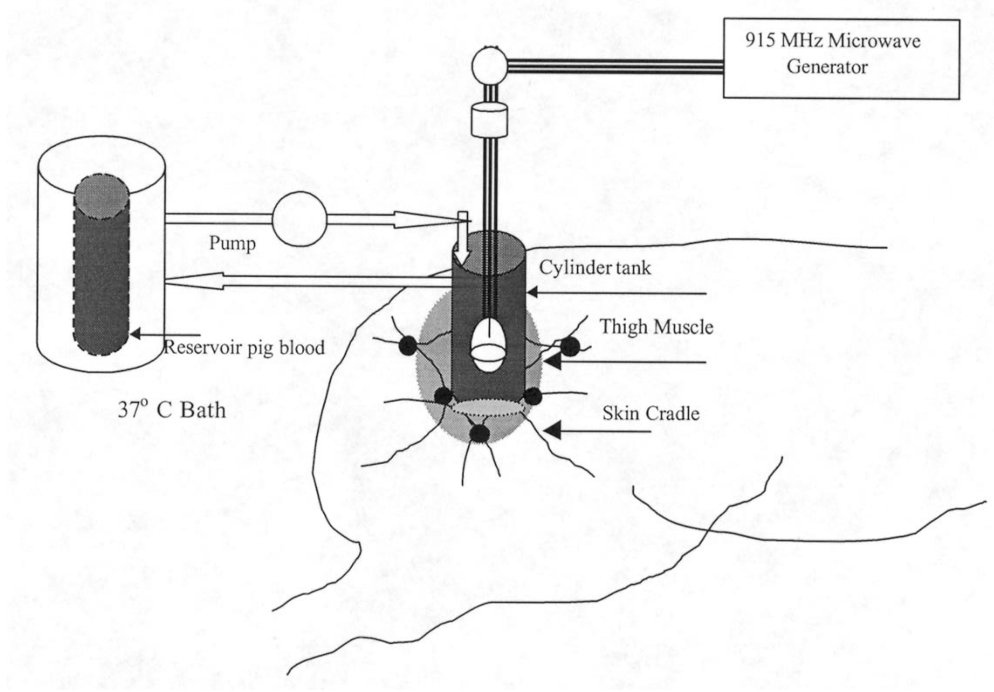

Fig. 8. Schematic drawing of the thigh muscle model. The skin and superficial muscle were dissected, exposing underlying facial later. A cylindrical tank was filled with heparinized pig blood at 36 °C–37 °C and flow was maintained at 20 ml/min.

of temperature rise and lesion growth during microwave ablation. Fig. 7 shows the experimental setup. We first created a perfused pig heart model to simulate the endocardial environment present in catheter ablation. The model consisted of a sectioned pig heart block suspended in a 4 cm $\times$ 3 cm $\times$ 2 cm polystyrene chamber. A perfusion pump controlled flow across the surface of each heart block, simulating blood flow. Four temperature sensors were inserted into each heart block, spaced 5 mm apart.

For each experiment, power was applied for 60 s. The temperature was recorded, the phantom was allowed to cool down for several minutes, the four sensors were withdrawn, the pig heart block was replaced, and the thermometry system was recalibrated. Once the phantom returned to equilibrium within 0.5 °C of initial conditions, the procedure was repeated. Ten tests were performed under identical treatment conditions in order to average unavoidable uncertainties in output power, heating time, and position of the antenna, catheters, and temperature probes. These were repeated for each power level.

Once a lesion is created, the effects are clearly irreversible, and new unexposed tissue must be used for testing. However, in contrast to RF ablation, there was no noticeable input impedance change or heating rate change due to the lesion formation. Reflected power remained nominal in all experiments for all power levels. This is partly due to lack of tissue charring, but also due to the microwave power deposition mechanism, which relies less on material conduction characteristics.

C. *In Vivo* Tests On Pig Thigh Muscle Model

The experimental setup for the *in vitro* tests on thigh muscle model is shown in Fig. 8. The methods employed for the wide-aperture spiral antenna were the same used by Nakagawa [19] for RF electrode tests. These studies were performed to accumulate sufficiently detailed temperature data and compare the tissue temperature at the border zone of irreversible tissue injury.

Five male pigs weighting between 77–89 kg were studied. As tested in the *in vitro* experiment, the catheter was positioned perpendicular to the thigh muscle, and held in contact with the exposed thigh muscle at a constant pressure by use of a custom balance. Tissue temperature was measured with the same fluoroptic probes as used in *in vitro* tests. Two thermal sensor probes were bundled together with shrink tubing. One sensor tip extended 3 mm from the end of the shrink tubing, and the other sensor tip extended 6.0 mm. The sensor probes were inserted into the muscle (3.0 and 6.0 mm from the surface) directly adjacent to the edge of the balloon–tissue interface. An additional fluoroptic temperature probe was attached at the center of the balloon–tissue interface.

Eight to ten applications of microwave energy were delivered to separate sites on the right thigh muscle. The skin incision was closed, the pig was turned onto its right side, and 8–10 applications of microwave energy were delivered at separate sites on the left thigh muscle. Microwave energy was delivered for 60 s using one of three power levels, i.e., 50, 100, or 150 W. Finally, the lesion was stained and its volume was determined by assuming it had an oblate spheroidal shape with volume given by

$$V = \left[\frac{4}{3}\pi A^2 C\right] \Big/ 2$$

where A and C represent the surface radius and the depth of the volume, respectively. For 60 s heating with 50-, 100-, and 150-W input power, the resulting lesion volumes were 260, 1200, and 1900 mm^3, respectively. The relationship is

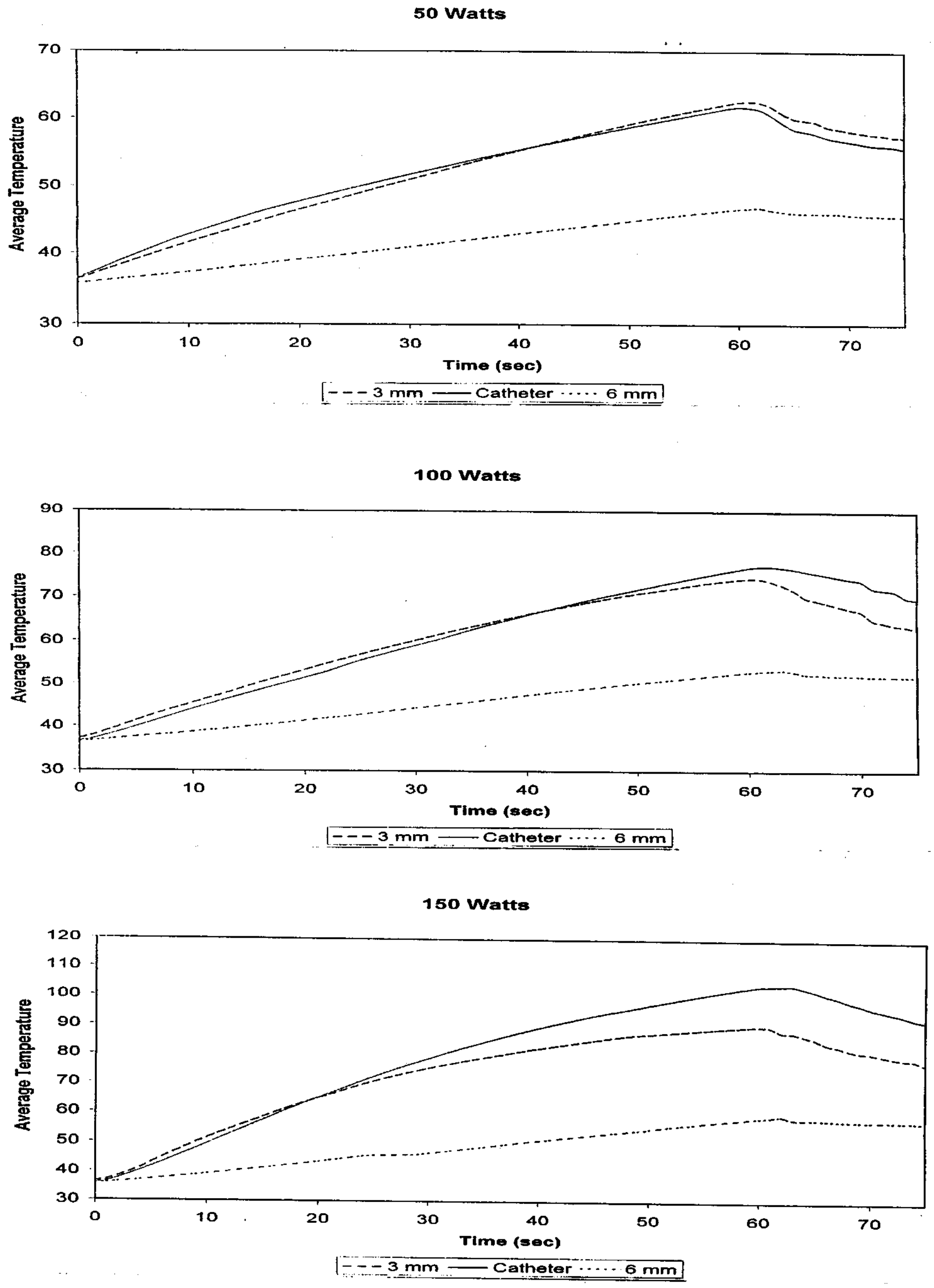

Fig. 9. Time course of lesion formation *in vivo* with various applied powers for 60-s microwave ablation.

not linear because the power deposition dependence is not linear with volume, and lesions created by heating tissue to above a particular temperature threshold do not have uniform temperature throughout.

In the thigh muscle model, a total of 70 lesions were produced, 23 lesions created at 50 W, 24 lesions at 100 W, and 24 lesion at 150 W. For each power level, the peak and average temperatures declined as a function of depth. At 100 W the peak temperature declined from 78.7 °C ±9.9 °C at the antenna–tissue interface to 73.4 °C ± 12.9°C and 55.5 °C ±6.6 °C at 3- and 6-mm deep, respectively. The average temperature versus time course for the lesion formation is shown in Fig. 9. The peak and average temperatures increased significantly as a function of power. The peak surface temperature recorded at the antenna–tissue interface is as low as 65.9 °C ±15.6 °C at 50 W and rises to 106.6 °C ±9.1 °C at 150 W. Similar relationships were observed for the average temperatures. Fig. 10 shows the lesions produced with various applied powers. Note that, although the measured power patterns of Fig. 4 indicate a ring of higher power, thermal conduction fills in the center of the ring to produce a convex lesion volume.

D. In Vivo Experiments On Open-Chest Pig Hearts

The experiment preparation for this animal test is similar to that described in the *in vivo* thigh muscle model experiment. Eight anesthetized pigs weighing between 70–90 kg were

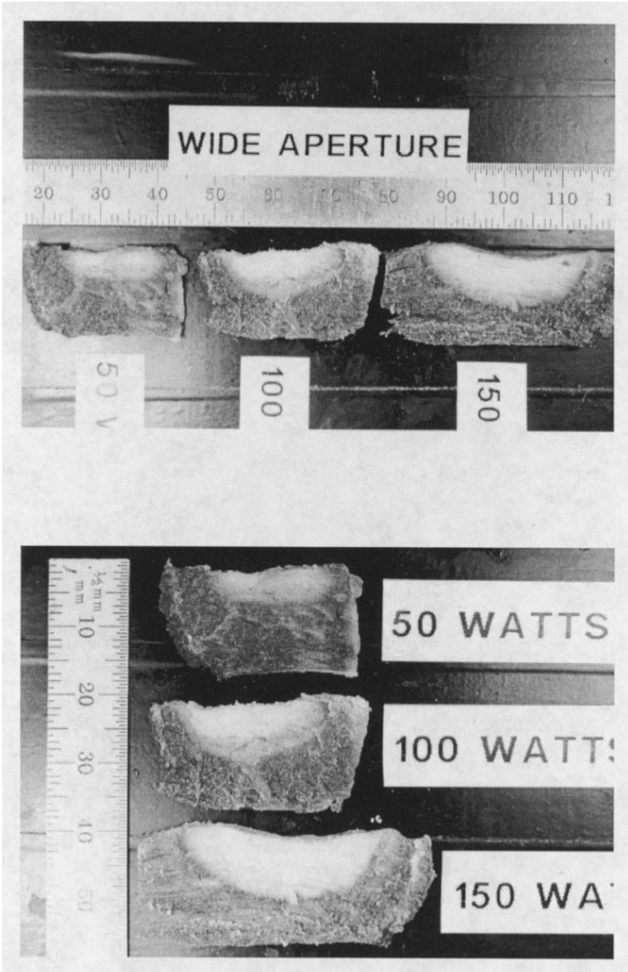

Fig. 10. Representative *in vivo* from thigh muscle model lesions produced with various applied power levels.

Fig. 11. Lesion generated by 60-s duration, 150-W power application, normal view, from the open-chest model.

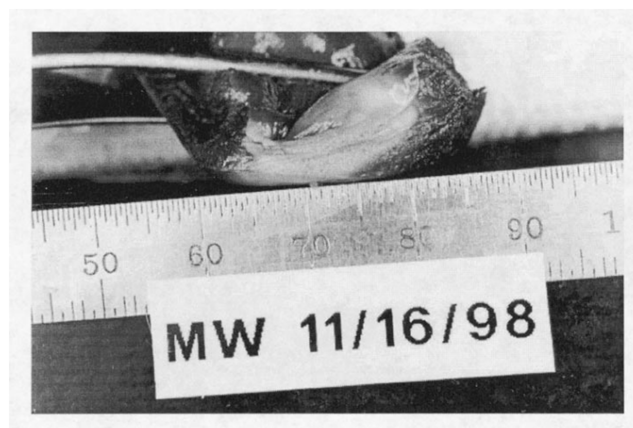

Fig. 12. Transmural lesion generated by 60 s duration, 150 W power application, depth view, from the open-chest model.

studied. A surface electrocardiogram was continually recorded during each procedure. A sternotomy incision was made to expose the heart and the pericardium was incised. The catheter was inserted into the left ventricle, and guided by fluoroscope, brought into contact with the left ventricle apex. Microwave power of 150 W was then delivered to the tissue for 60 s. After completion of the experiments, the pigs were sacrificed, the hearts were removed, and the lesions were examined.

In the open-chest experiment, a total of ten lesions were produced, with one or two lesions created on each pig. Figs. 11 and 12 show the representative lesions. Note that the lesions are transmural and that there is no charring of surface tissue. The depths produced are sufficient for the ablation of an arrythomogenic focus that is very deep within the ventricular myocardium or is subepicardial.

IV. Conclusions

The wide-aperture spiral antenna design is based on effectively delivering power in cardiac tissue to create a wide deep oblate spheroidal lesion. The spiral antenna is well matched to biological tissue at the operating frequency of 915 MHz. The antenna design is demonstrated in phantom tissue by measuring the reflection parameter S_{11} and transmission parameter S_{21}, and by comparing them to those of a monopole antenna. Full-power heating experiments at 50, 100, and 150 W on *in vitro* and *in vivo* animal tissue indicate that the field patterns in phantom combined with thermal conduction effects generate the desired lesion shape. These results show that the wide-aperture microwave spiral antenna design is capable of creating lesions of significant depth that may be applicable for the ablative therapy of ventricular tachycardia.

While all of the experiments reported were performed with a rigid spiral antenna, work is proceeding on a collapsible version that will be introduced through blood vessels. In addition, practical enhancements, including fluid cooling of the coaxial feed cable, co-locating mapping electrodes and feed wires, and catheter steering mechanisms are being perfected.

Acknowledgment

The authors wish to thank Prof. C. Vittoria, Northeastern University, Boston, MA, for assistance with the measurements of reflection coefficient, K. Warner, Massachusetts Institute of Technology (MIT) Lincoln Laboratories, Lexington, MA, for the power instrumentation, and A. W. Morgenthaler, Northeastern University, Boston, MA, for many helpful discussions.

REFERENCES

[1] W. Jackman *et al.*, "Catheter ablation of atrioventricular junction using radiofrequency current in 17 patients. Comparison of standard and large-tip electrode catheters," *Circulation*, vol. 83, p. 1562, 1991.

[2] J. Langberg *et al.*, "Ablation of atrioventricaular junction using radiofrequency energy using a new electrode catheter," *Amer. J. Cardiol.*, vol. 67, p. 142, 1991.

[3] A. Rosen and H. Rosen, Eds., *New Frontiers in Medical Device Technology*. New York: Wiley, 1995.

[4] F. Morady *et al.*, "Radiofrequency catheter ablation of ventricular tachycardia in patients with coronary artery disease," *Circulation*, vol. 87, pp. 363–372, 1993.

[5] Y. Kim *et al.*, "Treatment of ventricular tachycardia by transcatheter radiofrequency ablation in patients with ischemic heart disease," *Circulation*, vol. 89, pp. 1094–1102, 1994.

[6] J. Langberg *et al.*, "Catheter ablation or the atrioventricular junction using a helical microwave antenna: A novel means of coupling energy to the endocardium," *PACE*, vol. 14, pp. 2105–2133, 1991.

[7] R. Nevels, G. Dickey, F. Arndt, G. Raffoul, J. Carl, and A. Pacifico, "Microwave catheter design," *IEEE Trans. Biomed. Eng.*, vol. 45, pp. 885–890, July 1998.

[8] L. N. Horowitz, A. H. Harken, J. A. Kastar, and M. E. Josephson, "Ventricular resection guided by epicardial and endocardial mapping for treatment of recurrent ventricular tachycardia," *New Eng. J. Med.*, vol. 302, p. 590, 1980.

[9] C. H. Durney, "Electromagnetic field propagation and interaction with tissues," in *An Introduction to the Practical Aspects of Clinical Hyperthermia*, S. B. Field and J. W. Hand, Eds. New York: Taylor & Francis, 1990, ch. 10.

[10] J. G. Whayne, S. Nath, and D. E. Haines, "Microwave catheter ablation of myocardium *in vitro*: Assessment of the characteristics of tissue heating and injury," *Circulation*, vol. 89, no. 5, pp. 2390–2395, May 1994.

[11] B. A. VanderBrink, Z. Gu, V. Rodriguez, M. S. Link, M. K. Homoud, N. A. M. Estes, III, C. M. Rappaport, and P. J. Wang, "Microwave ablation using a wide-aperture antenna design in a porcine thigh muscle preparation: *In vivo* assessment of temperature profile and geometry," *J. Cardiovas. Electrophys.*, vol. 11, no. 2, pp. 192–198, Feb. 2000.

[12] L. S. Taylor, "Electromagnetic syringe," *IEEE Trans. Biomed. Eng.*, vol. BME-25, pp. 303–304, May 1978.

[13] J. W. Strohbehn, E. W. Bowers, J. E. Walsh, and E. B. Douple, "An invasive antenna for locally induced hyperthermia for cancer therapy," *J. Microwave Power*, vol. 14, pp. 339–350, 1979.

[14] T. Satoh and P. R. Stauffer, "Implantable helical coil microwave antenna for interstitial hyperthermia," *Int. J. Hyperthermia*, vol. 4, no. 5, pp. 497–512, 1988.

[15] T. Wonnell, P. Stauffer, and J. Langberg, "Evaluation of microwave and radio frequency catheter ablation in a myocardium-equivalent phantom model," *IEEE Trans. Biomed. Eng.*, vol. 39, pp. 1086–1095, Oct. 1992.

[16] C. M. Rappaport, Z. Gu, and P. J. Wang, "Wide-aperture microwave catheter-based cardiac ablation," in *Progress Electromag. Res. Symp. Dig.*, Hong Kong, Jan. 1997, p. 316.

[17] Z. Gu, C. M. Rappaport, P. J. Wang, and B. A. VanderBrink, "A 2 1/4 turn spiral antenna for catheter cardiac ablation," *IEEE Trans. Biomed. Eng.*, vol. 46, pp. 1480–1482, Dec. 1999.

[18] A. W. Guy, "Analysis of electromagnetic fields induced in biomedical tissues by thermographic studies on equivalent phantom models," *IEEE Trans. Microwave Theory Tech.*, vol. MTT-19, pp. 205–214, Feb. 1971.

[19] H. Nakagawa and W. S. Yamanashi *et al.*, "Comparison of *in vivo* tissue temperature profile and lesion geometry for radiofrequency ablation with a saline-irrigated electrode versus temperature control in a canine thigh muscle preparation," *Circulation*, vol. 91, pp. 2264–2273, 1995.

Zeji Gu received the B.S. and M.S. degrees from the Beijing Broadcasting Institute, Beijing, China, in 1983 and 1988, respectively, both in electrical engineering, and the Ph.D. degree in electrical engineering from Northeastern University, Boston, MA, in 2000.

From 1990 to 1993, he was an RF Engineer and Lecturer at the Beijing Broadcasting Institute. In 1993, he was with Siemens China, Beijing, China, as a Systems Engineer. In 1994, he was with AT&T China Inc., he was a System Engineer. He is currently a Senior Design Engineer at Alpha Industries Inc., Woburn, MA, where he designs, develops, and tests monolithic microwave integrated circuits for wireless applications. His research interests include RF/microwave circuits, microwave antenna and biomedical applications, computational electromagnetics, and electromagnetic interference.

Carey M. Rappaport (S'80–M'87–SM'96) received the S.B. degree in mathematics, the S.B., S.M., and E.E. degrees in electrical engineering, and the Ph.D. in electrical engineering from the Massachusetts Institute of Technology (MIT), Cambridge, in 1982 and 1987, respectively.

From 1981 to 1987, he was a Teaching and Research Assistant at MIT. During the summers from 1981 to 1987, he was with the COMSAT Laboratories, Clarksburg, MD, and The Aerospace Corporation, El Segundo, CA. In 1987, he joined the faculty of Northeastern University, Boston, MA, where he is currently a Professor of electrical and computer engineering. During Fall 1995, he was Visiting Professor of electrical engineering at the Electromagnetics Institute, Technical University of Denmark, Lyngby, Denmark, as part of the W. Fulbright International Scholar Program. He has consulted for Geo-Centers Inc., PPG Inc., and several municipalities on wave propagation and modeling, and microwave heating and safety. He is Co-Principal Investigator of the Center for Subsurface Sensing and Imaging Systems (CenSSIS) Engineering Research Center. He has authored over 160 technical journal and conference papers in the areas of microwave antenna design, electromagnetic scattering computation, and bioelectromagnetics, and holds two reflector antenna patents and one biomedical device patent.

Dr. Rappaport is a member of Sigma Xi and Eta Kappa Nu. He was the recipient of the 1985 IEEE Antenna and Propagation Society (IEEE AP-S) H. A. Wheeler Award for Best Applications Paper.

Paul J. Wang, photograph and biography not available at time of publication.

Brian A. VanderBrink, photograph and biography not available at time of publication.